

Non-ST elevation myocardial infarction and post-stenting ventricular septal defect in the setting of viral myocarditis

Lilia M. Sierra-Galan¹, Angel L. Alberto-Delgado^{1,2}, Ana-Camila Flores-Ventura^{1,3}, Eugenio A. Ruesga-Zamora¹, Raquel Mendoza-Aguilar¹, Victor A. Ferrari⁴

¹American British Cowdray Medical Center, Mexico City, Mexico; ²Central Military Hospital, Mexico City, Mexico; ³Radiology Clinic, Diagnostic's Hospital, San Salvador, Salvador; ⁴Cardiovascular Division, Perelman School of Medicine, Hospital of the University of Pennsylvania, Philadelphia, PA, USA

Correspondence to: Lilia M. Sierra-Galan. Av. Carlos Graef Fernandez 154, room 207. Colonia Tlaxala, Delegacion Cuajimalpa, American British Cowdray Medical Center, Santa Fe Campus, Mexico City 05300, Mexico. Email: lilisierra@wdevel.net.

Submitted Feb 21, 2017. Accepted for publication Apr 07, 2017.

doi: 10.21037/cdt.2017.04.01

View this article at: <http://dx.doi.org/10.21037/cdt.2017.04.01>

Case presentation

A 58-year-old hypercholesterolemic male presented to the emergency room (ER) with palpitations, fatigue and shortness of breath. He was afebrile with an irregular heart rate (80–90 bpm), BP of 92/70 mmHg, respirations of 20/min, and an otherwise unremarkable physical examination. ECG showed atrial fibrillation (Afib) with mean heart rate of 80–90 bpm, left ventricular hypertrophy (LVH) and non-ischemic appearing ST elevation diffusely (*Figure 1A*), and he was admitted to the intensive care unit (ICU). Supplemental oxygen and intravenous fluids were given with excellent response. There were no signs or symptoms of infection. Troponin-I was 1,491.30 pg/mL. Transthoracic echo (TTE) showed mild LVH with normal left ventricular (LV) ejection fraction (EF) and segmental left anterior descending (LAD) territory hypokinesis with a normal pericardium. The working diagnosis was recent onset Afib with unstable angina. As an intermediate risk symptomatic patient, he underwent coronary computed tomography angiography (CCTA) (1). Despite controlled Afib, a 64-MDCT scan was diagnostic, and a coronary calcium score was 76 [62nd percentile, i.e., low probability of obstructive coronary artery disease (CAD)]. CCTA showed a partially calcified mild proximal LAD stenosis (CAD-RADS 2) (2) and a non-calcified moderate mid-LAD stenosis (CAD-RADS 3) (*Figure 1B*) (2). A resting mid-inferoseptal segment perfusion defect was seen, corresponding to the mid-LAD lesion (*Figure 1C,D*). Per guidelines (3), the patient underwent invasive conventional angiography (ICA)

confirming the CCTA findings, and mid-LAD stenting was performed (*Figure 1E-G*). A septal perforator and a diagonal branch were occluded during stenting, causing hemodynamically instability and heart failure requiring pharmacological support. C-reactive protein (CRP) and troponin-I peaked at 20.8 mg/dL and 5,064 pg/mL, respectively. The magnitude of the troponin level seemed out of proportion to the CAD findings and he underwent cardiac MR (CMR) to exclude myocarditis. CMR demonstrated mild LV dysfunction (LVEF 49%) with mid-LAD territory hypokinesis and normal RV function with an LV stroke volume of 87 mL. Imaging at the mid ventricular inferoseptal segment suggested a small ventricular septal defect (VSD) (*Figure 2, Figure 3 and Figure 4A-F*), a CMR-calculated Qp:Qs of 1.2, mild mitral regurgitation, and a small pericardial and pleural effusion. Tissue characterization sequences suggested myocardial edema in the mid inferoseptal segment, with several late gadolinium enhancement (LGE) patterns: an ischemic area corresponding to a mid-LAD subendocardial infarction; an area of non-ischemic origin suggestive of myopericarditis; and a third region matching the VSD area described in the cine images (*Figures 4G-I*). Two days post-CMR, CRP decreased to 16.8 mg/dL, but his heart failure increased with a brain natriuretic peptide (BNP) of 829 pg/mL. Based on the CMR and laboratory results and his hemodynamic state, the patient was treated for viral myopericarditis in the setting of ischemic heart disease and acute subendocardial myocardial infarction (MI). No precordial murmur was detected. His

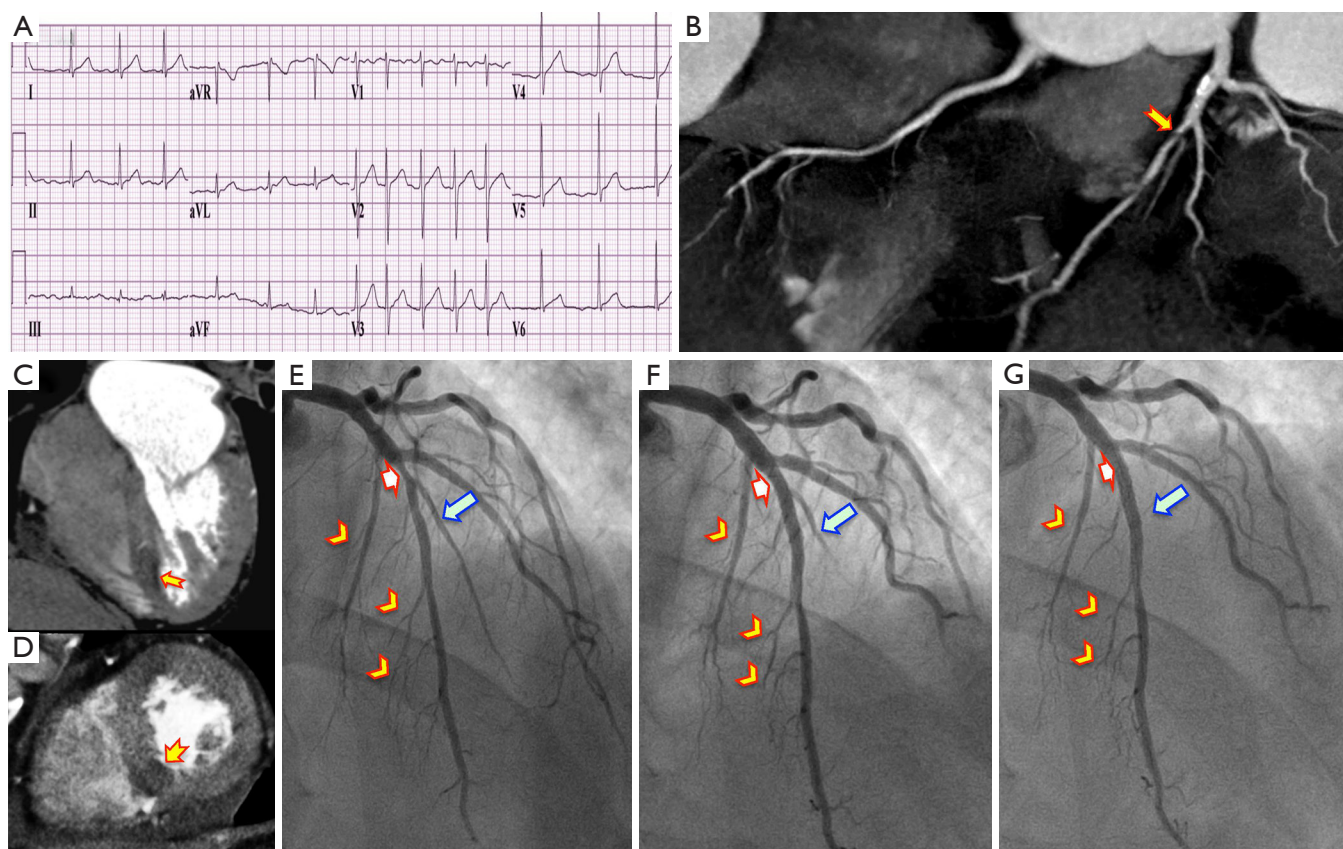


Figure 1 Twelve-lead ECG, cardiac computed tomographic angiography (CCTA) and invasive angiography. (A) Twelve-lead ECG demonstrating atrial fibrillation with a mean ventricular rate response of 80–90 bpm, left ventricular hypertrophy and non-ischemic appearing ST elevation in almost all leads; (B) a CCTA-extended 2D thin MIP showing a non-calcified moderate stenosis (CAD-RADS 3) in the mid-LAD (arrow) and a partially calcified mild stenosis (CAD-RADS 2) in the proximal LAD; (C) contrast enhanced-CT (from CCTA) 4-chamber view and mid-ventricular short axis view (D) that shows a resting perfusion defect in the mid left ventricular inferior septum (arrow). (E–G) Invasive angiography of the left coronary system in cranial anteroposterior projection. (E) corresponds to the significant mid-LAD lesion (white-red arrow), a second diagonal branch (blue arrow) and small tiny septal sub-branches (yellow-red arrow heads); (F) a post-PCI image shows the stented area with no residual lesion (white-red arrow), a partially occluded second diagonal branch (blue arrow) with only its proximal segment remaining, and the missing small septal sub-branches, likely occluded at its origin (yellow-red arrow heads); (G) final angiographic result showing a good post stenting result in the mid-LAD (white-red arrow), a missing second diagonal branch (blue arrow) and the missing small septal sub-branches or even occluded from its origin (yellow-red arrow heads). MIP, maximum intensity projection.

attending physician decided not to repair the muscular VSD due to his critical state and its restrictive nature, he improved slowly, and was discharged in good condition. During follow up, the patient intentionally lost weight, started a cardiac rehabilitation program, was compliant with his ischemic heart disease and heart failure treatments, and at 1-year follow-up is New York Heart Association (NYHA) functional class I.

The cause of his myopericarditis was Coxsackie virus sub-types B2, B4, B5 and B6, with titers indicative of recent infection.

Discussion

Post-MI VSD is a rare complication of acute MI. In the pre-thrombolytic era, its incidence was 1–2% (6), and has become less frequent, (0.17% to 0.31%) (7–9), due to improvements in acute reperfusion strategies (8); resulting in increased TIMI 3 flow, improved salvage index, and less haemorrhagic transformation of the infarcted myocardium (10). This case is interesting since despite significant improvements in mortality for peri-infarction



Figure 2 CMR. SSFP-with parallel and single-shot acquisition short axis mid ventricular view that shows an intramural linear hyperintense area within the inferoseptal and inferior segments that fills with blood during diastole (4).

Available online: <http://www.asvide.com/articles/1489>



Figure 3 CMR. Color-encoded phase contrast sequence velocity mapping sequence in the 4-chamber long axis view, demonstrating a systolic jet next to the mid-ventricular septum corresponding to the flow through the restrictive VSD (5).

Available online: <http://www.asvide.com/articles/1490>

management, the outcome of VSD post-MI remains poor reaching 41–80% mortality (7-10). Clinical presentations are variable depending on the size of the defect and associated factors such as RV infarction, ischemia or stunning, varying from hemodynamic stability to complete circulatory collapse (10) or death; our case had initial hemodynamic instability that resolved with pharmacological

and ventilatory support.

Reports of long-term survival are rare (10), however, our patient is in NYHA class I 1 year following the event. Two recognized time periods exist for these events: an early phase that occurs in the first 24 h (as in our case) and is related to a dissection of an intramural hematoma or hemorrhage into ischemic myocardium (10); and a second phase at 3 to 5 days. The former is the mechanism in our patient as well depicted by CCTA. The vascular territory corresponding to the mid-LAD lesion showed a resting transmural perfusion defect, a well-documented capability of CT (11). This was also well depicted by CMR (but not by echo), and showed a serpiginous defect within the mid-ventricular inferoseptal myocardium that matched the CCTA-demonstrated ischemic myocardium. The acute left to right shunt caused transient hemodynamic compromise, but was below threshold for detection by conventional echo. LGE by CMR demonstrated a small subendocardial LAD territory infarction, which was not large enough to compromise regional wall motion of that vascular territory, and therefore not detected by conventional echo; but which was confirmed by troponin-I and myoglobin. This case provides important learning points: (I) that myocarditis can coexist with ischemic heart disease (12,13), serving as an important inflammatory substrate complicating a typically low-risk percutaneous coronary intervention (PCI); (II) that in cases of myocarditis, CMR differentiates LGE patterns involving other pathophysiological mechanisms that elucidates the clinical diagnosis and offers better treatment options and outcomes to patients; (III) that CCTA should be considered as it demonstrates not only the presence and significance of CAD, but also associated resting perfusion defects; and (IV) that multimodality imaging is often complementary, more accurately depicts the clinical scenario and diagnosis, and results in clear patient benefit.

The co-existence of these pathological entities is possible, yet extremely rare, and increases patient risk. Clinicians should consider this clinical scenario when facing a complex myocarditis requiring vasoactive pharmacological and ventilatory support. The use of CCTA and CMR is strongly recommended to better define the pathological substrate, which can avoid unnecessary invasive procedures that place the life of the patient at risk and delay treatment, such as an endomyocardial biopsy (12,13).

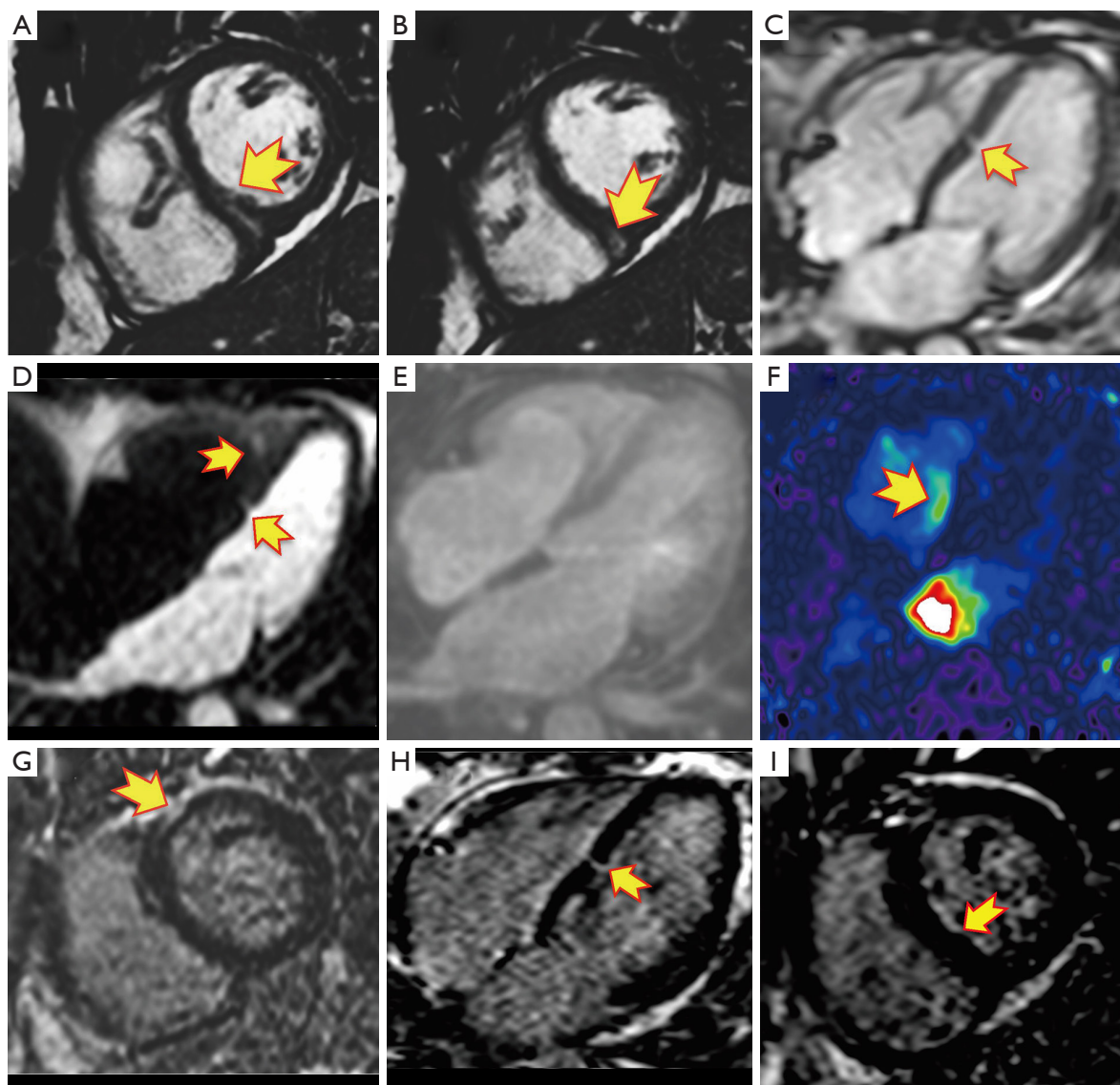


Figure 4 CMR study. (A) SSFP-with parallel and single-shot acquisition short axis mid ventricular diastolic image depicting an intramural linear hyperintense area within the inferoseptal and inferior segments (arrow) that extends (B) to the next slice level as a more circular structure within the inferior segment (arrow). The signal intensity of the described images (arrows) is similar to the blood pool; (C) SSFP-with parallel and single-shot acquisition long axis 4-chamber view image showing a small linear defect in the mid ventricular inferior septum (arrow); (D) single frame of a first pass perfusion sequence in the long axis 4-chamber view timed such that all contrast media is in the left side of the heart, and showing a small linear ventricular septal defect in the mid ventricular septum (left sided arrow) and a linear hyperintense area with similar signal intensity to the left ventricular cavity blood pool, in the RV apical region (right sided arrow); (E) magnitude image of the phase contrast sequence in a 4-chamber long axis view as a reference to Figure (F) showing the corresponding color velocity map, demonstrating systolic flow adjacent to the mid-ventricular septum (arrow), and representing the flow through the restrictive VSD; (G) single-shot-LGE in the short axis mid ventricular plane that shows epicardial linear intramural LGE of the anterior and anteroseptal segments (arrow) and hyperenhancement of the pericardium; (H) single-shot-LGE long axis 4-chamber view demonstrating a small linear defect in the mid ventricular inferior septum (arrow), very subtle endocardial hyperenhancement in basal and mid ventricular segments, and hyperenhancement of the pericardium; (I) single-shot-LGE in the short axis mid ventricular plane that shows endocardial LGE of the anteroseptal and inferoseptal segments (arrow), and hyperenhancement of the pericardium.

Acknowledgements

None.

Footnote

Conflicts of Interest: The authors have no conflicts of interest to declare.

References

1. Taylor AJ, Cerqueira M, Hodgson JM, et al. ACCF/SCCT/ACR/AHA/ASE/ASNC/NASCI/SCAI/SCMR 2010 appropriate use criteria for cardiac computed tomography. A report of the American College of Cardiology Foundation Appropriate Use Criteria Task Force, the Society of Cardiovascular Computed Tomography, the American College of Radiology, the American Heart Association, the American Society of Echocardiography, the American Society of Nuclear Cardiology, the North American Society for Cardiovascular Imaging, the Society for Cardiovascular Angiography and Interventions, and the Society for Cardiovascular Magnetic Resonance. *J Am Coll Cardiol* 2010;56:1864-94.
2. Cury RC, Abbara S, Achenbach S, et al. Coronary Artery Disease - Reporting and Data System (CAD-RADS): An Expert Consensus Document of SCCT, ACR and NASCI: Endorsed by the ACC. *JACC Cardiovasc Imaging* 2016;9:1099-113.
3. Task Force Members, Montalescot G, Sechtem U, et al. 2013 ESC guidelines on the management of stable coronary artery disease: the Task Force on the management of stable coronary artery disease of the European Society of Cardiology. *Eur Heart J* 2013;34:2949-3003.
4. Sierra-Galan LM, Alberto-Delgado AL, Flores-Ventura AC, et al. SSFP-with parallel and single-shot acquisition short axis mid ventricular view that shows an intramural linear hyperintense area within the inferoseptal and inferior segments that fills with blood during diastole. *Asvide* 2017;4:181. Available online: <http://www.asvide.com/articles/1489>.
5. Sierra-Galan LM, Alberto-Delgado AL, Flores-Ventura AC, et al. Color-encoded phase contrast sequence velocity mapping sequence in the 4-chamber long axis view, demonstrating a systolic jet next to the mid-ventricular septum (arrow) corresponding to the flow through the restrictive VSD. *Asvide* 2017;4:182. Available online: <http://www.asvide.com/articles/1490>.
6. Birnbaum Y, Fishbein MC, Blanche C, et al. Ventricular septal rupture after acute myocardial infarction. *N Engl J Med* 2002;347:1426-32.
7. Moreyra AE, Huang MS, Wilson AC, et al. Trends in incidence and mortality rates of ventricular septal rupture during acute myocardial infarction. *Am J Cardiol* 2010;106:1095-100.
8. López-Sendón J, Gurfinkel EP, Lopez de Sa E, et al. Factors related to heart rupture in acute coronary syndromes in the Global Registry of Acute Coronary Events. *Eur Heart J* 2010;31:1449-56.
9. French JK, Hellkamp AS, Armstrong PW, et al. Mechanical complications after percutaneous coronary intervention in ST-elevation myocardial infarction (from APEX-AMI). *Am J Cardiol* 2010;105:59-63.
10. Jones BM, Kapadia SR, Smedira NG, et al. Ventricular septal rupture complicating acute myocardial infarction: a contemporary review. *Eur Heart J* 2014;35:2060-8.
11. Gupta M, Kadakia J, Jug B, et al. Detection and quantification of myocardial perfusion defects by resting single-phase 64-slice cardiac computed tomography angiography compared with SPECT myocardial perfusion imaging. *Coron Artery Dis* 2013;24:290-7.
12. Feng WH, Lin TH, Su HM, et al. Fulminant myocarditis complicated with obstructive ST-elevation myocardial infarction--a rare case report. *Am J Emerg Med* 2013;31:635.e1-3.
13. Fujita S, Okamoto R, Takamura T. Fulminant myocarditis in a patient with severe coronary artery disease. *J Cardiol Cases* 2014;9:15-7.

Cite this article as: Sierra-Galan LM, Alberto-Delgado AL, Flores-Ventura AC, Ruesga-Zamora EA, Mendoza-Aguilar R, Ferrari VA. Non-ST elevation myocardial infarction and post-stenting ventricular septal defect in the setting of viral myocarditis. *Cardiovasc Diagn Ther* 2017;7(2):230-234. doi: 10.21037/cdt.2017.04.01